

Fully Memristive Spiking-Neuron Learning Framework and Its Applications on Pattern Recognition and Edge Detection

Zhiri Tang, Yanhua Chen, Shizhuo Ye, Ruihan Hu, Qijun Huang and Sheng Chang, *Senior Member, IEEE*

Abstract—Fully memristive spiking-neuron learning framework, which uses drift and diffusion memristor models as axon and dendrite respectively, becomes a hot topic recently with the development of memristor devices. Normally, some other devices like resistor or capacitor are still necessary on recent works of fully memristive learning framework. However, theoretically, one neuron needs axon and dendrite only, which makes technique process simpler and learning framework more similar to biologic brain. In this paper, a fully memristive spiking-neuron learning framework is introduced, in which a neuron structure is just built of one drift and one diffusion memristive models. To verify it merits, a feedforward neural network for pattern recognition and a cellular neural network for edge detection are designed. Experiment results show that compared to other memristive neural networks, our framework's the processing speed is much faster and the hardware resource is saved in pattern recognition due to its simple structure. Further due to the dynamic filtering function of diffusion memristor model in our learning framework, its peak signal noise ratio (PSNR) is much higher than traditional algorithms in edge detection.

Index Terms — fully memristive spiking-neuron, feedforward neural network, pattern recognition, cellular neural network, edge detection

I. INTRODUCTION

Memristor, which was postulated by L.O. Chua [1] in 1971, is the fourth basic circuit element alongside with resistor (R), inductor (L) and capacitor (C). After HP Labs practiced memristors by TiO_2 [2] in 2008, various memristors are pointed out. In general, memristors can be divided into two main types [3]: drift memristor and diffusion memristor while a regular neuron in human brain always consists of two main parts [4]: axon and dendrite. Axon, which is used as a channel for transmitting spiking signals [5], can be mimicked by drift memristor [6], and dendrite, which is used as a receptor that receives spiking signals from the previous neuron [7], can be mimicked by diffusion memristor [8]. Based on above analogy, fully memristive neuron, which uses drift and diffusion memristor as axon and dendrite respectively, has become a candidate for simulating biologic

neurons and realizing spike timing-dependent plasticity (STDP) [9]-[11] learning rules. Memristive neurons can form memristive neural networks, which have immense potential applications in many areas including high performance computing [12]-[14], pattern recognition [15]-[17] and edge detection [18]-[20] because of their advantages, such as fewer types of device, relatively simple technique process, and more close to biologic brain neuron [21].

Some state-of-the-art works about memristive neural networks for pattern recognition, such as unsupervised memristive crossbar structure [22] and feedforward memristive neural network [23], were also reported. Some other state-of-the-art works for edge detection were mainly memristive cellular neural networks [24]-[25] and multilayer perceptron with memristor crossbar [26].

However, how to use fully memristive learning framework is still an open area. One research on fully memristive neural network built a memristive crossbar by drift memristors, diffusion memristors and capacitors [22] while another research used memristors and metal-oxide-semiconductor field effect transistors (MOSFET) [27]. From above one can see that some other devices are still needed. Originally, drift and diffusion memristor should be merged into a basis neuron structure naturally and this neuron should use spiking signals as the information [28] which is transmitted between neurons. Hence, novel memristive spiking-neuron learning framework needs to be developed, which should be a recyclable structure for multilayer networks aiming to various applications.

Inspired by the above, this paper designs a fully memristive spiking-neuron learning framework using drift and diffusion memristor models only and applies it in pattern recognition and edge detection. The main contributions can be summarized as follows:

- A fully memristive spiking-neuron learning framework is designed. Only drift and diffusion memristor models are used to build a spiking-neuron structure without any other electron devices. This framework only needs the most basic memristive characteristics and uses spiking time information in learning process directly, which is friendly and universal for various memristors.
- A fully memristive feedforward neural network is designed based on the spiking-neuron, which can obtain the result of pattern recognition accurately. Due to the simple and direct spiking coding mode in the learning framework, it can reduce the hardware resource occupancies significantly and improve the processing speed quite efficiently.

This work was supported by the National Natural Science Foundation of China (61874079 and 61574102), the Fundamental Research Fund for the Central Universities, Wuhan University (2042017gf0052), the Wuhan Research Program of Application Foundation and Frontier Technology (2018010401011289), and the LuoJia Young Scholars Program. Part of calculation in this paper has been done on the supercomputing system in the Supercomputing Center of Wuhan University.

Zhiri Tang, Shizhuo Ye, Ruihan Hu, Qijun Huang and Sheng Chang are with the School of Physics and Technology, Wuhan University, Wuhan, 430072, China. Yanhua Chen is with State Key Laboratory of Information Engineering in Surveying, Mapping and Remote Sensing (LIESMARS), Wuhan University, Wuhan, 430072, China. (E-mail: gerinetang@whu.edu.cn; changsheng@whu.edu.cn).

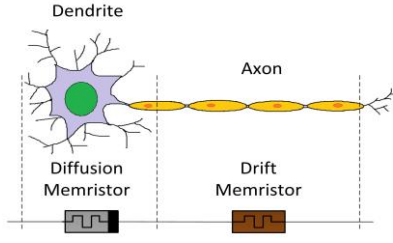


Fig. 1. Basic structure of neuron including drift and diffusion memristor models.

- c. A fully memristive cellular neural network is designed for edge detection based on the spiking-neuron. As the diffusion memristor model in the learning framework has dynamic filtering function, it can get a high peak signal to noise ratio (PSNR) of system and has a good performance on edge detection including classic images and complex remote sensing images.

II. FULLY MEMRISTIVE SPIKING-NEURON LEARNING FRAMEWORK

In this section, a fully memristive spiking-neuron learning framework is introduced, including how the drift and diffusion memristor models connect, how spiking information transmit between neurons and why this framework can mimic biologic neuron better.

A. Basic Structure of Spiking-Neuron

Current research show that drift and diffusion memristor models can mimic characteristics of axon and dendrite well, respectively. Hence, the memristive spiking-neuron structure obeys this law, which is shown as Fig. 1.

When the hold time of input spikes are the same, we can use the basis diffusion memristor model [29] as follow:

$$\begin{cases} I_{\text{output}}(t) = U_{\text{input}}, & U_{\text{input}} > \text{Threshold} \\ I_{\text{output}}(t) = 0, & U_{\text{input}} < \text{Threshold} \end{cases} \quad (1)$$

The diffusion memristor model can be seen as a threshold switch to determine whether a spike from the previous neuron was worth firing back.

For drift memristor in traditional HP model, the relationship of the voltage at the two ends of the memristor and its current is

$$U(t) = [R_{\text{off}} - (R_{\text{off}} - R_{\text{on}})\mu_v] \frac{R_{\text{on}}}{D^2} \int_{-\infty}^t I(t)dt \quad (2)$$

So the drift memristor value is

$$M_{\text{drift}}(t) = R_{\text{off}} - (R_{\text{off}} - R_{\text{on}})\mu_v \frac{R_{\text{on}}}{D^2} \int_{-\infty}^t I(t)dt = k_1 - k_2 \int_{-\infty}^t I(t)dt \quad (3)$$

where $k_1 = R_{\text{off}}$ and $k_2 = (R_{\text{off}} - R_{\text{on}})\mu_v R_{\text{on}} / D^2$.

It can be seen that is linearly dependent on the amount of electricity (Q) flowing through it. The value of drift memristor is the reciprocal of synaptic weight in neuron, which can be increased or decreased during training process.

B. Unsupervised Learning Algorithm

In our learning framework, diffusion memristor model, dendrite, works as a threshold switch in neuron while the drift

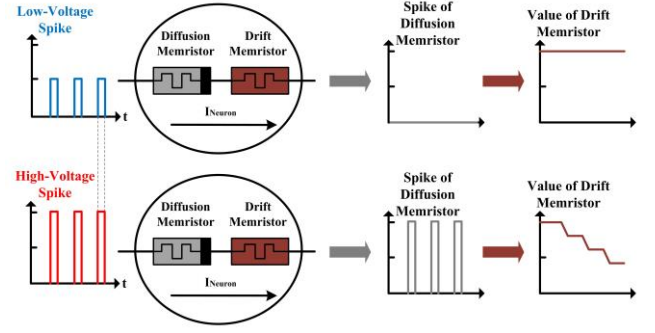


Fig. 2. Unsupervised learning algorithm of fully memristive spiking-neuron model.

memristor model, axon, serves as synaptic weight, which is shown as Fig. 2.

During the training process, high-voltage or low-voltage spikes are inputted to this neuron structure. When input is low, diffusion memristor won't response. When input is high, diffusion memristor will fire backward and the output spike of diffusion memristor is the same as the input spike, which will decrease the value of drift memristor. Since the value of drift memristor is the reciprocal of synaptic weight in neuron, the synaptic weight of this neuron will increase receiving the high-voltage spike.

$M_{\text{drift}i+1}$ is the value of drift memristor after one input spike, which is described as follow:

$$M_{\text{drift}i+1} = \begin{cases} k_1 - k_2 \frac{U_{\text{input}}}{M_{\text{drift}i}} t_{\text{spike}}, & U_{\text{input}} > \text{Threshold} \\ M_{\text{drift}i}, & U_{\text{input}} < \text{Threshold} \end{cases} \quad (4)$$

where $M_{\text{drift}i}$ is the value of drift memristor before the input spike. t_{spike} is the duration of this input voltage spike, which is very short so that the change value of drift memristor during the spike time can be ignored.

Considering the spikes are continuously inputted during training process, the synaptic weight of neuron with high input voltage will increase along with the increase number of input high-voltage spikes. The synaptic weight of neuron with low input voltage won't have any change. After training, the synaptic weights with high-voltage spikes are much higher than those with low-voltage spikes.

According to STDP, the more spikes between two neurons, the closer or thicker the connection between them. The neurotransmitters [30] give preference to the closer or thicker axon. In our framework, the value of drift memristor will decrease during the training process. The currents, like neurotransmitters, prefer the branch with lower memristor value. Hence, STDP's essence is realized in a simple and direct way.

In test process, the output currents from drift memristors vary after training. The currents of drift memristors with lower value, which means the higher synaptic weight, will be higher. Neurotransmitters, represented by electrical currents, prefer shorter or thicker paths. So a self-competitive process is built naturally. The synaptic weight is only determined by the input voltage, and it directly determines how much

TABLE I
COMPARISONS OF PROCESSING SPEED AND RESOURCE CONSUMPTION

Design	FPGA Platform	Process Speed (MHz)	Resource
DMS-ANN [31]	Cyclone II: EP2C70F672C6	N/A	3266 (LEs)
Our Network	Cyclone II: EP2C70F672C6	165.32	952 (LEs)
TC-Network [32]	Cyclone IV: EP4CE115	40.68	3031 (LEs)
Our Network	Cyclone IV: EP4CE115F23C9	96.67	951 (LEs)
HF-MNN [23]	Stratix V: 5SGXEA7N2F45C2	256.54	869 (in ALMs)
Our Network	Stratix V: 5SGXEA7N2F45C2	448.23	477 (in ALMs)

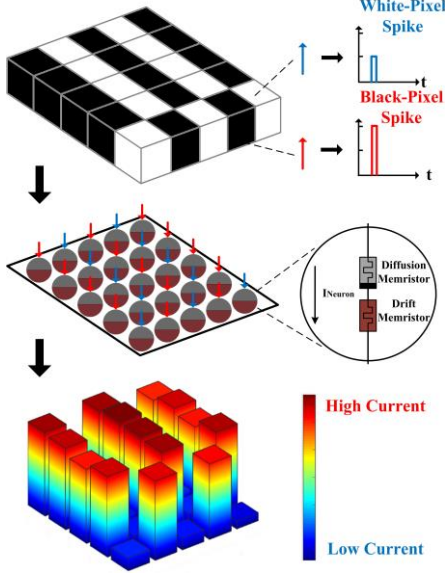


Fig. 3. The architecture of fully memristive feedforward neural network.

current it can ‘grab’. Following the STDP and self-competitive process, the learning algorithm of this neuron structure is unsupervised.

In this framework, only basic drift and diffusion memristor models are employed. All this neuron structure needs are the most elementary characteristics of memristor rather than special materials or particular structures. In other words, our learning framework is universal to various memristors.

III. FULLY MEMRISTIVE FEEDFORWARD NEURAL NETWORK FOR PATTERN RECOGNITION

To verify the merits of our learning framework such as simple connection mode and direct information representation by spiking signals, a fully memristive feedforward neural network for pattern recognition is designed within STDP unsupervised learning process in this section. The test results show that the network has extremely high processing speed and low resource maintaining the recognition accuracy.

A. Architecture of Network

The architecture of this network is shown as Fig. 3. The overall feedforward neural network is divided into three layers: the spikes input layer, the fully memristive spiking-neuron layer and the current output layer. First, the input images are coded into spikes, in which the white and black pixels are coded into low and high voltage spikes, respectively.

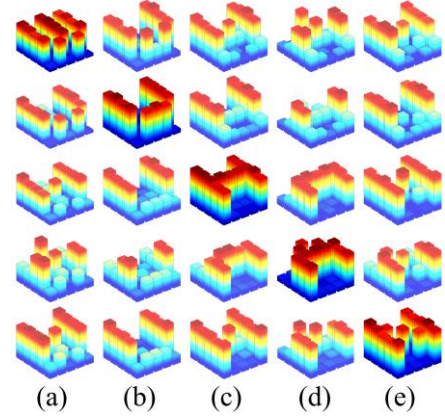


Fig. 4. Test results of 5*5 alphabet database ‘WUHAN’ with random noise (a) test results of alphabet ‘W’ (b) test results of alphabet ‘U’ (c) test results of alphabet ‘H’ (d) test results of alphabet ‘A’ (e) test results of alphabet ‘N’.

Second, in the fully memristive spiking-neuron layer, each pixel needs one fully memristive spiking-neuron. Given an example of a 5*5 pixels image, the number of neurons is 25. As mentioned above, the diffusion memristor is used as a threshold switch which is higher than white-pixel spike and lower than black-pixel spike. Hence the fully memristive spiking-neurons corresponding to black-pixels will ‘open’, which means the values of drift memristor models in these neurons will decrease and synaptic weights of these neurons will increase.

Third, in the current output layer, the output current values depend on the values of drift memristors. If a pixel is black, the drift memristor corresponding to this pixel will decrease during the training process. Then its output current value will be higher than the memristors corresponding to white-pixels.

In this network, the number of categories is the number of output spikes and the result of image classification can be obtained by comparing the sum of output current corresponding to each category directly. The one with the highest total output current, which means the one with the lowest total value of drift memristor, represents the correct classification.

B. Experimental Results and Analysis

A home-made 5*5 alphabet recognition database ‘WUHAN’ is used to test the performance of our fully memristive feedforward neural network. The test results with random noise on standard images are shown as Fig. 4. The five images of Fig. 4(a) are the output currents corresponding to the five types as the input test image is randomly noised ‘W’. It is clear that the first output image has the highest

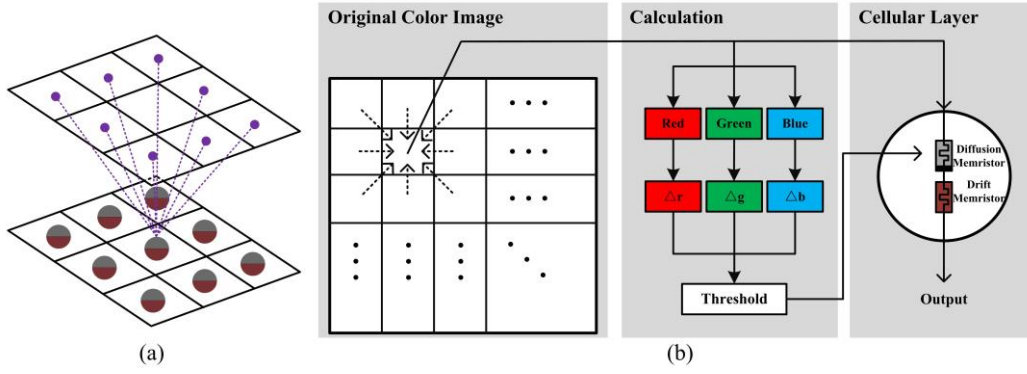


Fig. 5. The architecture of fully memristive cellular neural network (a) network connection mode (b) network flow.

current as it portrays the alphabet ‘W’, which is the correct classification result. Likewise, the noised alphabet ‘U’, ‘H’, ‘A’ and ‘N’ are correctly classified in Fig. 4(b), (c), (d) and (e), which shows good classification accuracy.

The fully memristive feedforward neural network is unsupervised and follows the STDP in a quite simple way. To verify the network’s performance, it is implemented by Field Programmable Gate Array (FPGA) and compared with an artificial neural network using a digital memristor simulator (DMS-ANN) [31], a two-compartment memristive network (TC-Network) [32] and a hardware friendly memristive neural network (HF-MNN) [23] with the same network scale on the same platform, respectively. Because TC-Network didn’t indicate specific FPGA platform, we select the slowest FPGA in the same series as TC-Network, which is Cyclone IV: EP4CE115F23C9. From the results in TABLE I, one can see our network gains high processing speed with low resource consumption, which is derived from its brief neuron connection mode and efficient spiking coding. Specially, our memristive learning framework eliminates other devices normally needed by memristive neural networks, so resource is saved. Since spiking information is directly dealt by fully memristive neuron structure ignoring additions and multiplications, processing speed is improved significantly.

IV. FULLY MEMRISTIVE CELLULAR NEURAL NETWORK FOR EDGE DETECTION

Since the diffusion memristors in our learning framework can be seen as dynamic filtering thresholds, a fully memristive cellular neural network for edge detection is designed to show our learning framework’s merits on anti-noise in this section. Besides it can achieve high PSNR with noised images, its edge detection results on complex objects, such as remote sensing images, are still quite good.

A. Architecture of Network

The basic idea comes from a phenomenon, which is known as the human eye’s strong adaptability to brightness varies and this adaptability depending on the current brightness. That means human eye cannot notice the brightness changes until the change goes beyond the specific threshold [33]. Utilizing this theory, edge detection methods can be developed. Some research have concluded the human eye’s detection thresholds for red, green, and blue respectively

based on current brightness values, which is shown as follow:

$$\Delta r = \begin{cases} 12734e^{-0.1494r}, & 0 \leq r < 38 \\ 5397e^{-0.1015r}, & 38 \leq r < 60 \\ 127300e^{[(0.07r-7.55)e^{0.026r}-0.089r]}, & 60 \leq r < 97 \\ 8.4569, & 97 \leq r \leq 255 \end{cases} \quad (5)$$

$$\Delta g = \begin{cases} 12734e^{-0.1494g}, & 0 \leq g < 38 \\ 5107.5e^{-0.1015g}, & 38 \leq g < 60 \\ 120470e^{[(0.07g-7.55)e^{0.026g}-0.089g]}, & 60 \leq g < 97 \\ 8.003, & 97 \leq g \leq 255 \end{cases} \quad (6)$$

$$\Delta b = \begin{cases} 12734e^{-0.1494b}, & 0 \leq b < 38 \\ 9101.6e^{-0.1015b}, & 38 \leq b < 60 \\ 241750e^{[(0.07b-7.55)e^{0.026b}-0.089b]}, & 60 \leq b < 97 \\ 14.2663, & 97 \leq b \leq 255 \end{cases} \quad (7)$$

where r , g and b are pixel values of red, green, and blue colors respectively, whose value ranges are from 0 to 255. Δr , Δg and Δb are respectively the minimum changes of red, green and blue that human eyes can recognize to color images. However, since the proportion of primary colors varies, some research [34] proposed a threshold $T_{i,j}$ for color images as follow:

$$T_{i,j} = \omega_r \Delta r_{i,j} + \omega_g \Delta g_{i,j} + \omega_b \Delta b_{i,j} \quad (8)$$

which has $\omega_r = 0.114$, $\omega_g = 0.587$ and $\omega_b = 0.299$.

According to above, our network architecture is shown as Fig. 5. In the process of edge detection, the minimum changes of three colors are calculated first according to the target pixel, and then the total thresholds are got. These thresholds are the switch thresholds of diffusion memristors in our network’s cellular layer.

The eight pixels around the target pixel are compared with the target pixel in turn. If the difference value exceeds the threshold value of diffusion memristor, it will fire backward and the value of drift memristor will decrease. If not, the diffusion memristor won’t fire and the value of drift memristor won’t change. The edge detection process is completed when all eight pixels are compared. After that, the same voltages are added to each neuron module in the cellular layer directly, just as we do above in pattern

TABLE II
COMPARISON OF PSNR AMONG SOME EDGE DETECTION ALGORITHMS

Test image	Sobel (dB)	Robert (dB)	Prewitt (dB)	Log (dB)	Canny (dB)	Our Network (dB)
Lena	13.6548	13.6593	13.6822	10.0023	8.5448	21.1933

TABLE III
ANTI-NOISE PERFORMANCE OF URBAN REMOTE SENSING IMAGES

	Airport	Commercial District	Football Field	Industrial District	Park	Parking Lot	Railway Station	Viaduct
PSNR(dB)	20.0930	19.6833	19.3321	19.5697	19.5116	19.4885	20.0409	20.1920

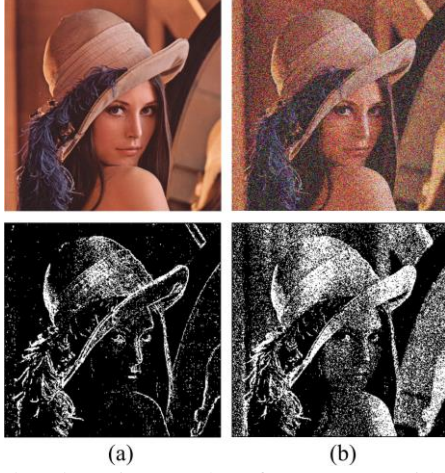


Fig. 6. Edge detection results of 'Lena' (a) without noise (b) with noise.

recognition. Finally, a diagram composed of the obtained output current can be got, which is the output image after edge detection.

B. Experimental Results and Analysis

The classic edge detection image 'Lena' with 512*512 pixels is used to test the anti-noise performance of our fully memristive cellular neural network as shown in Fig. 6(a). The diffusion memristors in the fully memristive cellular neural network act as dynamic filtering thresholds, which can increase the network's PSNR theoretically. Gauss noise with mean 0 and variance 0.1 is added to 'Lena' and the test results are given as Fig. 6(b). Compared to traditional algorithms such as Sobel, Robert, Prewitt, Log and Canny, the PSNR of our network is over 21dB and the highest of other traditional algorithms is below 14dB as shown in TABLE II.

To illustrate our network's performance in complex objects, a remote sensing image dataset with 600*600 pixels from Google satellite images, WHU-RS19 [35], is tested. This dataset is very suitable to verify a method's anti-noise capacity, because the edge information of urban remote sensing images are complex and significant, which are always with various noises. Specifically, we test eight different types of urban scenes, including airport, commercial district, football field, industrial district, park, parking lot, railway station and viaduct as shown in Fig. 7.

Due to the dynamic filtering function of diffusion memristor models in our network, the edge detection results of urban remote sensing images are very good. In Fig. 7(a), the edges of all the runways and terminals, even the location

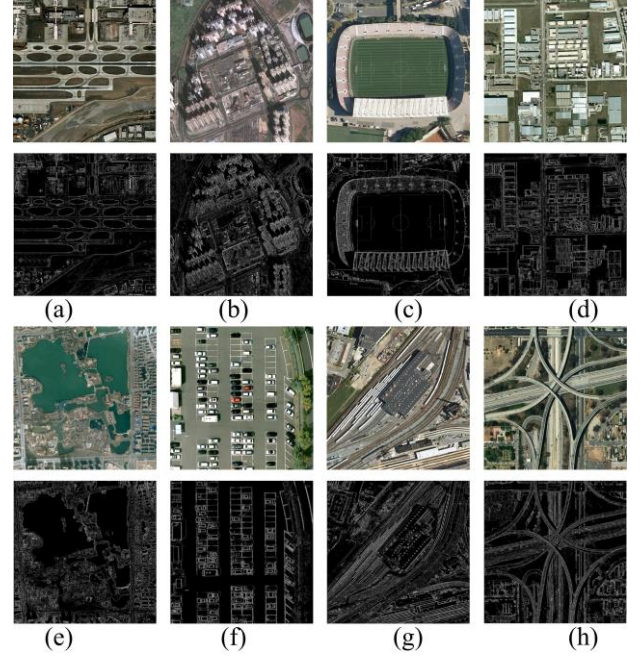


Fig. 7. Edge detection results of remote sensing images (a) airport (b) commercial district (c) football field (d) industrial district (e) park (f) parking lot (g) railway station (h) viaduct.

of airplanes are very clear. In Fig. 7(b), the edges of both the streets and the buildings are distinct. In Fig. 7(c), the edges of the stadium frames and the white lines on the court are distinguished and the green stripes on the court are filtered out. In Fig. 7(d), the edges of all farmlands and industrial buildings are obvious. In Fig. 7(e), the edges of lakes in park are clear which is helpful to distinguish the boundary between the lake and the road clearly. In Fig. 7(f), the edges of all parking lines and vehicles are very distinct which is helpful for people to distinguish whether there is a vehicle in this parking space or not. In Fig. 7(g), the edges of all the trains are appeared and even the number of trains in the railway station can be counted. In Fig. 7(h), the edges of all the viaducts are very clear and it can be distinguished which viaduct is higher and which is lower. To test the anti-noise performance of urban remote sensing images, the same Gauss noise on 'Lena' is added to these eight image types. The PSNR of noised images ranges from 19 to 22, which shows a good anti-noise performance as shown in TABLE III.

V. CONCLUSIONS

In this paper, a fully memristive spiking-neuron learning framework, which uses diffusion and drift memristor models

only, is presented. Due to its simple structure and fluent spiking information flow, this learning framework has many merits such as high processing speed, low resource and high anti-noise performance. These merits are verified by the learning framework's applications including a fully memristive feedforward neural network for pattern recognition and a fully memristive cellular neural network for edge detection. We hope this idea can give an inspiration for the developments of fully memristive neuron and neural networks, and other neuromorphic algorithms.

REFERENCES

- [1] L. O. Chua, "Memristor-the missing circuit element," *IEEE Transactions on Circuit Theory*, vol. 18, no. 5, 1971, pp. 507-519.
- [2] D.B. Strukov, G.S. Snider, D.R. Stewart and R.S. Williams, "The missing memristor found," *Nature*, vol. 453, no. 7191, 2008, pp. 80.
- [3] Q. Xia *et al.*, "Memristor-CMOS hybrid integrated circuits for reconfigurable logic," *Nano Letters*, vol. 9, no. 10, 2009, pp. 3640.
- [4] E.J. Huang and L.F. Reichardt, "Neurotrophins: roles in neuronal development and function," *Annual Review of Neuroscience*, vol. 24, no. 1, 2001, pp. 677-736.
- [5] M. Tessier-Lavigne and C.S. Goodman, "The molecular biology of axon guidance," *Science*, vol. 274, no. 5290, 1996, pp. 1123-1133.
- [6] B. Linaresbarranco and T. Serranogotarredona, "Memristance can explain Spike Time-Dependent Plasticity in Neural Synapses," *Nature Precedings*, 2009.
- [7] N. Toni, P.A. Buchs, I. Nikonenko, C.R. Bron and D. Muller, "LTP promotes formation of multiple spine synapses between a single axon terminal and a dendrite," *Nature*, vol. 402, no. 6760, 1999, pp. 421.
- [8] W. Adam *et al.*, "Synaptic behavior and STDP of asymmetric nanoscale memristors in biohybrid systems," *Nanoscale*, vol. 5, no. 16, 2013, pp. 7297-7303.
- [9] Linares-Barranco *et al.*, "On Spike Timing-Dependent Plasticity, Memristive Devices, and Building a Self-Learning Visual Cortex," *Frontiers in Neuroscience*, vol. 5, no. 26, 2011, pp. 26.
- [10] T. Serrano-Gotarredona, T. Masquelier, T. Prodromakis, G. Indiveri, and B. Linares-Barranco, "STDP and STDP variations with memristors for spiking neuromorphic learning systems," *Frontiers in Neuroscience*, vol. 7, no. 7, 2013, pp. 2.
- [11] X. Hu, S. Duan, G. Chen and L. Chen, "Modeling Affections with Memristor-Based Associative Memory Neural Networks," *Neurocomputing*, vol. 223, 2016, pp. 129-137.
- [12] L. Wang, H. Li, S. Duan, T. Huang and H. Wang, "Pavlov associative memory in a memristive neural network and its circuit implementation," *Neurocomputing*, vol. 171, 2016, pp. 23-29.
- [13] S.H. Jo *et al.*, "Nanoscale memristor device as synapse in neuromorphic systems," *Nano letters*, vol. 10, no. 4, 2010, pp. 1297-1301.
- [14] S. Duan, H. Wang, L. Wang, T. Huang and C. Li, "Impulsive Effects and Stability Analysis on Memristive Neural Networks With Variable Delays," *IEEE Transactions on Neural Networks & Learning Systems*, vol. 28, no. 2, 2017, pp. 476-481.
- [15] S. Duan, X. Hu, L. Wang, S. Gao and C. Li, "Hybrid memristor/RTD structure-based cellular neural networks with applications in image processing," *Neural Computing & Applications*, vol. 25, no. 2, 2014, pp. 291-296.
- [16] M. Hansen, F. Zahari, M. Ziegler and H. Kohlstedt, "Double-Barrier Memristive Devices for Unsupervised Learning and Pattern Recognition," *Frontiers in Neuroscience*, vol. 11, 2017, pp. 91.
- [17] X. Hu, G. Feng, S. Duan and L. Liu, "A Memristive Multilayer Cellular Neural Network With Applications to Image Processing," *IEEE Transactions on Neural Networks & Learning Systems*, vol. 28, no. 8, 2016, pp. 1889-1901.
- [18] S. Duan, X. Hu, Z. Dong, L. Wang and P. Mazumder, "Memristor-based cellular nonlinear/neural network: design, analysis, and applications," *IEEE Transactions on Neural Networks & Learning Systems*, vol. 26, no. 6, 2015, pp. 1202-1213.
- [19] L. Wang, X. Wang, S. Duan and H. Li, "A spintronic memristor bridge synapse circuit and the application in memristive cellular automata," *Neurocomputing*, vol. 167, 2015, pp. 346-351.
- [20] J. Zhou, J.J. Wu and Y.H. Tang, "Edge Detection of Binary Image Based on Memristors," *Advanced Materials Research*, vol. 791-793, 2013, pp. 2066-2070.
- [21] Z. Dong, L. Wang, L. Luo, X. Hu and S. Duan, "Multiple Memristor Series-Parallel Connections with Use in Synaptic Circuit Design," *IET Circuits Devices & Systems*, vol. 11, no. 2, 2017, pp. 123-134.
- [22] Z. Wang *et al.*, "Fully memristive neural networks for pattern classification with unsupervised learning," *Nature Electron*, vol. 1, 2018, pp. 137-145.
- [23] Z. Tang *et al.*, "A Hardware Friendly Unsupervised Memristive Neural Networks with Weight Sharing Mechanism," *Neurocomputing*, <https://doi.org/10.1016/j.neucom.2018.12.049>
- [24] G. Cserey, A. Rák, B. Jákli and T. Prodromakis, "Cellular neural networks with memristive cell devices," *Proc. IEEE International Conference on Electronics*, 2011.
- [25] E. Bilotta, P. Pantano and S. Vena, "Speeding Up Cellular Neural Network Processing Ability by Embodying Memristors," *IEEE Transactions on Neural Networks & Learning Systems*, vol. 28, no. 5, 2017, pp. 1228-1232.
- [26] C. Yakopcic and T.M. Taha, "Memristor crossbar based implementation of a multilayer perceptron," *Proc. IEEE National Aerospace & Electronics Conference*, 2018, pp. 38-43.
- [27] Rosenthal, S. Greshnikov, D. Soudry and S. Kvatinisky, "A fully analog memristor-based neural network with online gradient training," *Proc. IEEE International Symposium on Circuits & Systems*, 2016, pp. 1394-1397.
- [28] R. Hu, S. Chang, H. Wang, J. He and Q. Huang, "Efficient Multispike Learning for Spiking Neural Networks Using Probability-Modulated Timing Method," *IEEE Transactions on Neural Networks & Learning Systems*, 2018, pp. 1-14.
- [29] J.H. Yoon *et al.*, "An artificial nociceptor based on a diffusive memristor," *Nature Communications*, vol. 9, no. 1, 2018.
- [30] S.G. Amara and M.J. Kuhar, "Neurotransmitter transporters: recent progress," *Annual Review of Neuroscience*, vol. 16, no. 1, 1993, pp. 73-93.
- [31] V. Ntinis, I. Vourkas, A. Abusleme, G. C. Sirakoulis, A. Rubio, "Experimental study of artificial neural networks using a digital memristor simulator," *IEEE Transactions on Neural Networks & Learning System*, vol. 29, no. 10, 2018, pp. 5098-5110.
- [32] Q. Lin *et al.*, "The dynamical analysis of modified two-compartment neuron model and FPGA implementation," *Physica A Statistical Mechanics & Its Applications*, vol. 484, 2017.
- [33] J.A. Ferwerda, "Elements of early vision for computer graphics," *IEEE Computer Graphics & Applications*, vol. 21, no. 5, 2001, pp. 22-33.
- [34] S. Deng, Y. Tian, X. Hu, P. Wei and M. Qin, "Application of new advanced CNN structure with adaptive thresholds to color edge detection," *Communications in Nonlinear Science & Numerical Simulation*, vol. 17, no. 4, 2012, pp. 1637-1648.
- [35] G. Xia *et al.*, "Structural high-resolution satellite image indexing," *B. ISPRS TC VII Symposium - 100 Years ISPRS*, vol. 38, 2010, pp. 298-303.